A Novel Approach for Dielectric Constant Measurement Using Microwave Oscillators

Vikram Sekar, William J. Torke, Samuel Palermo and Kamran Entesari

Texas A&M University, College Station, TX 77843

***Abstract* — In this paper, planar microwave oscillators are used to measure the dielectric constant of organic liquids for the first time. Dielectric constant of an unknown material is calculated based on the change in oscillation frequency caused by the material-under-test (MUT). A split-ring resonator (SRR) is chosen as the sensing element due its small area and high confinement of electric fields which makes it sensitive to permittivity changes of the MUT above the SRR. A C-band microwave oscillator prototype is fabricated on RT/Duroid 5880 substrate and calibrated using ethanol and methanol as reference materials. The dielectric constant of small quantities (< 20µL) of acetic acid, xylene, isobutanol and ethyl acetate are extracted from measurement of oscillation frequency shift and show good agreement with previously reported values.**

***Index Terms* — Permittivity measurement, microwave oscillator, split-ring resonator.**

I. Introduction

Development of systems for accurate measurement of material properties is essential for a number of applications in industry, medicine, and pharmaceuticals [1]. For this purpose, several resonant techniques have been developed for permittivity characterization of unknown materials at a single microwave frequency. Traditionally, shift in resonant frequency of waveguide, dielectric or coaxial resonators have been used for material characterization due to their high sensitivity [2]. However, such devices are often bulky and expensive, which limits their use when low-cost, in-situ measurements need to be made. Recently, substrate-integrated-waveguide-based sensors have been proposed as a low-cost alternative with high sensitivity and medium size [3]. To overcome the issue of cost and size, microwave sensors using planar resonant structures have been implemented [4].

The resonant techniques in [2]-[4] rely on measuring the relative shift of the magnitude of S-parameters due to the material-under-test (MUT). This method has inherent limitations when materials with high dielectric loss at microwave frequencies (such as organic liquids) need to be characterized. The degradation of quality factor of the resonator due to a high-loss MUT results in a $|S_{21}|$ (or $|S_{11}|$) response that does not have a distinguishable peak (or notch) at any frequency. This makes it impossible to extract the dielectric constant of the MUT. To be able to detect high-loss materials using this technique, a reasonably high resonator quality factor must be maintained by reducing the sample volume of the high-loss MUT. As a result, the resonance frequency shifts caused by the MUT are drastically lower, which makes them hard to detect accurately [4].

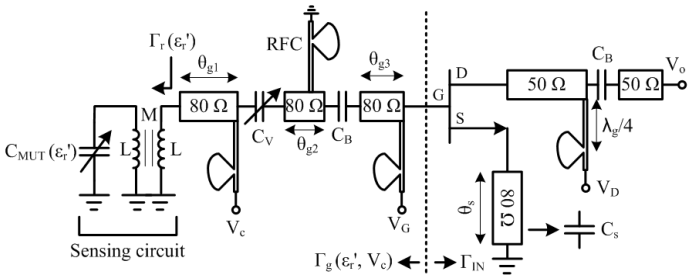

Fig. 1. Circuit schematic of a C-band permittivity sensing VCO.

In this paper, a novel approach to measure dielectric constant based on a C-band microwave oscillator is presented. Dielectric constant is detected based on shifts of oscillation frequency caused by the phase change of the sensing element when the MUT is applied. The proposed detection method is independent of the sample volume and loss of the MUT as long as oscillation conditions are satisfied and the frequency shift is detectable. The fabricated sensor prototype is used to successfully extract the dielectric constant of several organic liquids.

II. Sensing Oscillator Design

A. Schematic

Fig. 1 shows the circuit schematic of the C-band negative resistance oscillator employing a common source series feedback element to generate negative resistance. The active device is an Avago Technologies' ATF-36077 pseudomorphic high electron mobility transistor (pHEMT) biased at a drain-source voltage (V_{DS}) of 1.5 V and gate-source voltage (V_{GS}) of -0.2 V with a drain current (I_D) of 10 mA.

The gate network of the transistor consists of the sensing circuit which has a capacitor [$C_{MUT}(\varepsilon_r')$] coupled by a transformer to a transmission line, whose value of capacitance depends on the MUT. The change in complex reflection coefficient $\Gamma_r(\varepsilon_r')$ of the sensing circuit when the MUT is applied causes a change in the oscillation frequency (f_0). In order to control the oscillation frequency before the MUT is applied, an Aeroflex/Metelics MHV500 silicon hyper-abrupt tuning varactor (C_V) is included. The overall reflection coefficient looking into the gate network including the sensing circuit, varactor, 80-Ω transmission lines with electrical lengths θ_{g1}, θ_{g2} and θ_{g3}, and DC-blocking capacitor C_B (AVX Accu-P, 10 pF, 0402 size) is represented by $\Gamma_g(\epsilon_r', V_c)$.

978-1-61284-757-3/11/$26.00 C2011 IEEE

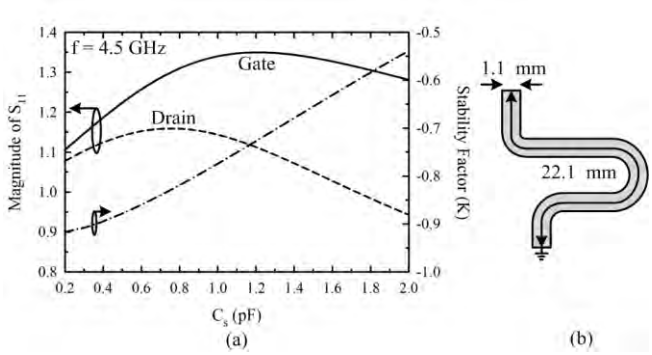

Fig. 2. (a) Simulated S_{11} parameters at gate and drain, and stability factor (K) for different source capacitances C_s. (b) Implementation of a 0.7 pF capacitor using an 80-Ω short circuited stub.

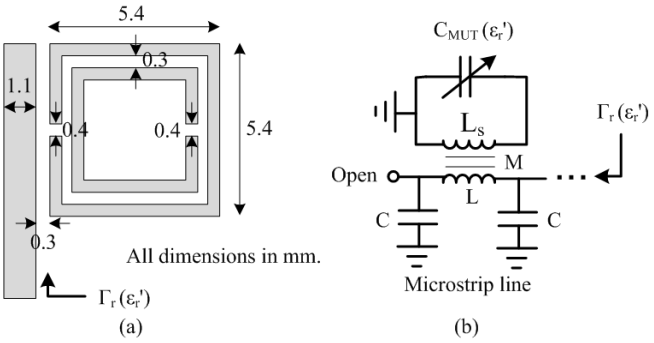

Fig. 3. (a) Implementation of the sensing circuit using a split-ring resonator (SRR). (b) Equivalent circuit model of the SRR coupled to a microstrip line.

The reflection coefficient looking into the gate of the transistor is represented as Γ_{IN}.

The source terminal of the transistor is connected to an 80-Ω short circuited stub with electrical length θ_s that provides the required capacitance (C_s) to generate instability, and provides a DC path to ground for biasing. The drain terminal of the transistor is connected to 50-Ω transmission lines with arbitrary length which is AC-coupled to the output using capacitance C_B. At all biasing points, RF-chokes (RFCs) are designed using fan-stubs and high-impedance $\lambda_g/4$-long (at f_0) transmission lines.

B. Series Feedback Network

To generate instability in the transistor for oscillation, the value of C_s must be adjusted so that the transistor provides a negative resistance looking into the gate, implying $|\Gamma_{IN}| > 1$. In other words, the Rollett's stability factor (K) must be made negative to ensure stable oscillations. Fig. 2(a) shows the simulated S_{11} parameter (at $f_0 = 4.5$ GHz) at the gate and drain terminals, and stability factor K, when different capacitor values (C_s) are connected to the source terminal of a properly biased transistor. Simulation is performed using Agilent Technologies' Advanced Design System (ADS) by employing the nonlinear model of the transistor present in the ADS design library.

The value of C_s is chosen so that magnitude of S_{11} at the gate and drain terminals is as high as possible, implying greatest negative resistance generation [5]. Choosing $C_s = 0.7$ pF results in $|S_{11}|$ values of 1.29 and 1.16 at the gate and drain terminals respectively, with a stability factor K = -0.84. Fig. 2 (b) shows the implementation of a 0.7 pF capacitor using an 80-Ω short circuited stub with electrical length $\theta_s = 302°$, where the transmission line is meandered to minimize the overall area. The short circuited stub also provides DC ground for the source of the transistor. The source capacitor is designed on Rogers RT/Duroid 5880 ($\epsilon_r = 2.2, h = 0.787$ mm) and dimensions are obtained from full-wave simulations in Agilent Momentum. For these parameters, the reflection coefficient looking into the transistor gate is $\Gamma_{IN} = 1.29\angle -43°$ at $f_0 = 4.5$ GHz. For stable oscillations, the gate network must be designed to meet the oscillation conditions given by [5]

$$\left|\Gamma_g(\epsilon_r', V_c)\right| \times |\Gamma_{IN}| > 1 \quad (1)$$

$$\angle\Gamma_g(\epsilon_r', V_c) + \angle\Gamma_{IN} = 0 \quad (2)$$

To resonate out the source capacitor and satisfy (2), the gate network must exhibit an overall inductive behavior.

C. Gate Network

Fig. 3 shows the implementation of the sensing circuit which consists of a split-ring resonator (SRR) coupled to a microstrip line with a mutual coupling coefficient M, and its equivalent circuit model [6]. The high confinement of electric fields at the open ends, and between the rings of the SRR makes it highly sensitive to permittivity changes in the dielectric layer above the SRR [7]. In addition, the area occupied by the SRR for a particular resonant frequency is much lesser due to its sub-wavelength nature [6].

Since the gate network must exhibit an overall inductive behavior, circuit area is minimized if $\Gamma_r(\epsilon_r')$ represents an inductance. Hence, the resonant frequency of the SRR ($f_{SRR} = 1/2\pi\sqrt{C_{MUT}(\epsilon_r')L_s}$) is chosen such that $f_{SRR} > f_0$, so that the SRR exhibits an equivalent inductance of $1/(1/L_s - \omega_0{}^2 C_{MUT}(\epsilon_r'))$ at $f = f_0$. The capacitance C_{MUT} (ϵ_r') is predominantly due to the capacitance between the two rings of the SRR and at the open gaps of the two rings, which changes when a MUT with relative permittivity ϵ_r' is placed on top of the SRR. The equivalent inductance of the rings (L_s) only depends on the relative permeability μ_r of the MUT [6], and μ_r=1 for nonmagnetic MUTs considered here. For the dimensions shown in Fig. 3(a), the SRR in the absence of an MUT has a resonant frequency of $f_{SRR} = 5.5$ GHz.

To provide independent control of the oscillation frequency, the voltage-controlled varactor C_v (V_c) is included in the gate circuit. Providing independent frequency control is essential in future development of a phase-locked loop based measurement system to detect changes in oscillation frequency without employing an external spectrum analyzer, and is explained in detail in the conclusion. In the absence of

978-1-61284-757-3/11/$26.00 C2011 IEEE

the MUT (ε_r'=1), the entire gate network including the sensing circuit, varactor, DC blocking capacitors, RFCs and transmission lines are simulated in Agilent Momentum, and the electrical lengths θ_{g1}, θ_{g2} and θ_{g3} (Fig. 1) are adjusted so that conditions (1) and (2) are satisfied for a particular varactor voltage V_c. The optimized electrical lengths of the transmission lines are $\theta_{g1} = 100°$, $\theta_{g2} = 9.4°$ and $\theta_{g3} = 11°$. Substrate-scaled equivalent models for DC blocking capacitors are used to include all parasitic effects of surface-mount components in full-wave simulation. For these values, the reflection coefficient looking into the gate network is $\Gamma_g(\epsilon_r' = 1, V_c = 0\,V) = 1\angle 43°$ which satisfies (1) and (2).

The choice of f_{SRR} is made based on the sample volumes of MUT that intend to be used, and the physical distance of the sensing circuit from other oscillator components. If a higher value of f_{SRR} is chosen, then the area of the SRR is smaller, and hence smaller samples of MUT are required to cover the sensor area. However, choosing a higher value of f_{SRR} implies that the sensing circuit is more inductive at f_0. Hence, the length of transmission lines $\theta_{gi}(i = 1,2,3)$ must be made smaller to compensate for the extra inductance of the sensing circuit. As a result, the sensing circuit might be very close to the surface-mount components of the oscillator. This makes it hard to construct a sample-well around the SRR to contain the MUT. Here, choosing $f_{SRR} = 5.5$ GHz provides an optimum trade-off between physical distance and sample quantity.

III. Fabrication and Measurements

The oscillator designed in Sec. II is fabricated on Rogers RT/Duroid 5880 with ϵ_r'=2.2 and thickness 0.787 mm using conventional PCB etching technology. Fig. 4(a) shows the fabricated sensor prototype. In order to contain the MUT, a sample well is constructed using a 5 mm long polypropylene tube ($\epsilon_r' = 2.2$) with a wall thickness of 1 mm and inner diameter of 5 mm. To prevent sensor degradation due to interaction between the MUT and sensor surface, one end of the tube is closed by gluing a thin sheet of polyethylene teraphalate (PET) ($\epsilon_r' = 2.5, \tan\delta = 0.025$) with a thickness of 0.1 mm to the tube. The other end of the tube is open so that the MUT can be dispensed into the sample well. Fig. 4(b) shows the spectrum of the oscillator measured using an Agilent E4446A spectrum analyzer without the MUT and has a single tone at 4.4222 GHz with an output power of -5 dBm.

To calibrate the sensor, oscillation frequency shifts caused by well-known materials are measured for known sample volumes. Using the dielectric constant values of the calibration materials in [8] at 4.5 GHz, a 2nd-order polynomial is curve-fit to the frequency shifts. Figs. 5(a) and 6(a) show the curve-fit polynomial obtained from frequency shifts caused by 10μL and 20μL samples of ethanol and methanol (with 99.8% purity), respectively. Frequency shift is measured by averaging the oscillator spectrum ten times to reduce the frequency error caused by drift. The oscillator drift is in the order of ±150 kHz (over a 5 min. period) and does

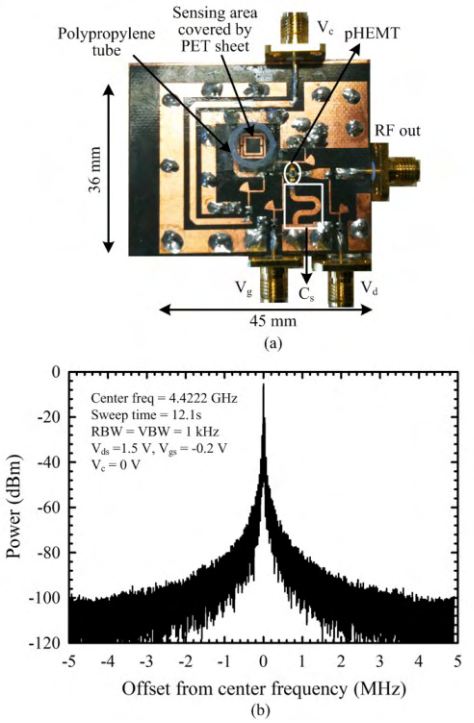

Fig. 4. (a) Photograph of the fabricated permittivity-sensing oscillator prototype. (b) Measured oscillation spectrum without MUT.

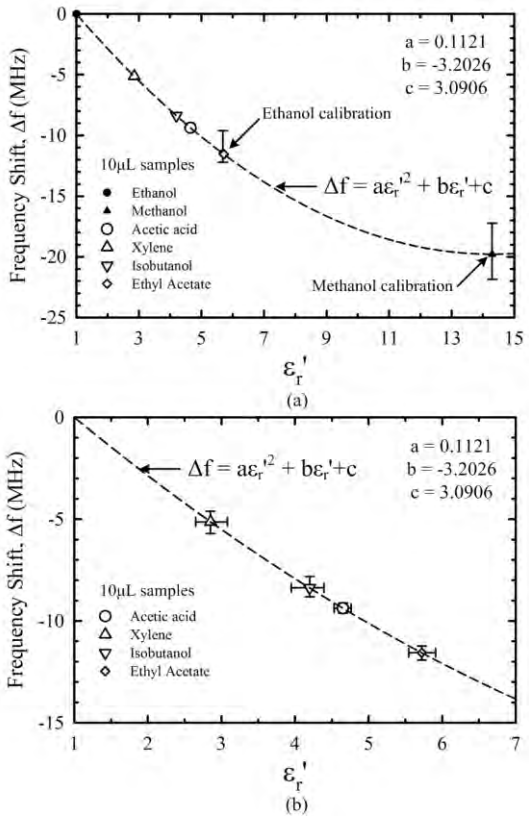

Fig. 5. (a) Measured oscillator frequency shift versus ε_r' for 10μL MUT samples. Error bars are shown only for calibration materials. (b) Error in measurement of MUTs for 10μL sample volumes. In both graphs, plotted symbols depict mean values.

978-1-61284-757-3/11/$26.00 C2011 IEEE

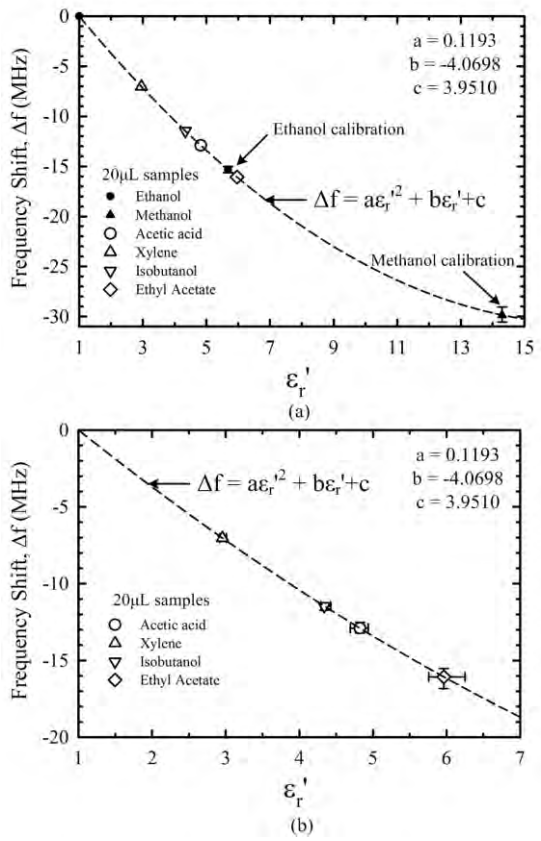

Fig. 6. (a) Measured oscillator frequency shift versus ε_r' for 20μL MUT samples. Error bars are shown only for calibration materials. (b) Error in measurement of MUTs for 20μL sample volumes. In both graphs, plotted symbols depict mean values.

not significantly affect the sensor accuracy which typically shows shifts of >5MHz for the 10μL and 20μL samples of MUTs considered here. Five measurements are taken for each sample volume of each calibration material, and the average values are used for curve fitting. Using a larger sample volume results in lower error in the curve-fitting coefficients, and hence better detection accuracy because higher sample volumes cover the whole sensor area in a repeatable fashion.

Next, 10μL and 20μL samples of MUTs such as acetic acid, xylene, isobutanol and ethyl acetate (all with >99.5% purity) are applied to the oscillator and the frequency shifts for each material is obtained by averaging the oscillator spectrum ten times. Five measurements are taken for each sample volume of each MUT. Figs. 5(a) and 6(a) show the average frequency shifts obtained for different MUTs for 10μL and 20μL sample volumes, respectively. The dielectric constant of the MUT for a given volume is extracted by inverting the curve-fitted polynomial equation for that particular volume. Figs. 5(b) and 6(b) show the error in measured frequency shift and dielectric constant for 10μL and 20μL sample volumes of MUT, respectively. The error in the coefficients obtained by curve-fitting during calibration are not considered here. The extracted values of dielectric constant for each MUT is summarized in Table I, and show good agreement with the values reported in [8].

TABLE I
COMPARISON BETWEEN REPORTED AND MEASURED DIELECTRIC CONSTANT OF MATERIALS AT 4.5 GHZ.

Material	ε_r' (Reported) [8]	ε_r' (Meas)-10μL	ε_r' (Meas)-20μL
Ethanol	5.68	-	-
Methanol	14.30	-	-
Acetic Acid	4.72	4.65 ± 0.11	4.82 ± 0.08
Xylene	2.55	2.85 ± 0.17	2.95 ± 0.05
Isobutanol	3.94*	4.19 ± 0.20	4.33 ± 0.08
Ethyl Acetate	6.06+	5.72 ± 0.18	5.96 ± 0.20

* At 1.8 GHz and drops to ε_r'=3.4 at 8 GHz [3].
+ At 3.0 GHz but only drops to ε_r'=5.81 at 9 GHz due to its low dispersion.

IV. CONCLUSION

A novel approach to measure the dielectric constant of liquid materials using planar microwave oscillators has been presented for the first time. Extraction of the dielectric constant of several organic liquids show good agreement with reported values. Although the sensor proposed here utilizes a spectrum analyzer for measurement, the authors are currently working on incorporating the sensing oscillator into a phase-locked loop. In this way, any changes in oscillation frequency can be negated by changing the control voltage (V_c) of the oscillator. The change in V_c can be easily stored digitally using an analog-to-digital converter, and mapped into changes in the dielectric constant of the MUT. Such a system is completely self-sustained and requires only a DC power supply, and is very useful where portability is important.

REFERENCES

[1] E. Nyfors and P. Vainikainen, *Industrial Microwave Sensors*. Norwood, MA: Artech House, 1989.

[2] L. F. Chen, C. K. Ong, C. P. Neo, V. V. Varadan and V. K. Varadan, *Microwave Electronics: Measurement and Materials Characterization*. New York: Wiley, 2004.

[3] K. Saeed, R. D. Pollard and I. C. Hunter, "Substrate integrated waveguide cavity resonators for complex permittivity characterization of materials," *IEEE Trans. of Microw. Theory and Tech.*, vol. 56, no. 10, pp. 2340-2347, October 2008.

[4] K. Saeed, A. C. Guyette, I. C. Hunter and R. D. Pollard, "Microstrip resonator technique for measuring dielectric permittivity of liquid solvents and for solution sensing," *IEEE MTT-S Interna. Microw. Symp.*, pp.1185-1188, 3-8 June 2007.

[5] P. G. Wilson and R. D. Carver, "An easy-to-use FET DRO design procedure suited to most CAD programs," *IEEE MTT-S Microwave Symp. Dig.*, vol. 3, pp. 1033–1036, June 1999.

[6] J. D. Baena, *et al.*, "Equivalent-circuit models for split-ring resonators and complementary split-ring resonators coupled to planar transmission lines," *IEEE Trans. on Microw. Theory and Tech.*, vol. 53, no. 4, pp. 1451-1461, April 2005.

[7] H-.J. Lee and J-.G. Yook, "Biosensing using split-ring resonators at microwave regime," Applied Phys. Lett., 92, 254103, 2008.

[8] F. Buckley and A. A. Maryott, "Tables of dielectric dispersion data for pure liquids and dilute solutions," NBS circular 589, National Institute of Standards and Technology (NIST), 1958.

978-1-61284-757-3/11/$26.00 C2011 IEEE